



ESA/Contract No. 4000126561/19/I-NB

Consortium Members



ESA Sea Level CCI+

# Product Validation and Inter Comparison Report

Reference:

Nomenclature: SLCCI+\_PVIR\_018\_ProductValidation

Issue: 3.0

Date: Dec. 11, 25



**Chronology Issues:**

Issue:	Date:	Reason for change:	Author
1.0	02/03/20	Initial Version	NOC, LEGOS, CLS
2.0	30/07/21	Annual update	NOC, LEGOS, CLS
2.1	03/09/21	Improvements after review comments	NOC, LEGOS, CLS
2.2	10/03/22	Update with v2.1 results (sections 2, 3.1)	NOC, LEGOS, CLS
2.3	14/06/23	Validation results of the v2.2 dataset	LEGOS, CLS
3.0	11/12/25	Validation results of the v3.0 dataset	LEGOS, CLS

**People involved in this issue:**

Written by:	A. Cazenave, L Leclercq, L Tolu		
Checked by:	JF Legeais (CLS)		
Approved by:	JF Legeais (CLS)	11/12/2025	

**Acceptance of this deliverable document:**

Accepted by ESA:	S. Connors (ESA)		
------------------	------------------	--	--

**Distribution:**

Company	Names	Contact Details
ESA	S. Connors, M. Restano	<a href="mailto:Sarah.Connors@esa.int">Sarah.Connors@esa.int</a> ; <a href="mailto:Marco.Restano@esa.int">Marco.Restano@esa.int</a>
CLS	J.-F. Legeais ; P. Prandi ; A Mangilli ; V Quet	<a href="mailto:jlegeais@groupcls.com">jlegeais@groupcls.com</a> ; <a href="mailto:pprandi@groupcls.com">pprandi@groupcls.com</a> ; <a href="mailto:amangilli@groupcls.com">amangilli@groupcls.com</a> ; <a href="mailto:vquet@groupcls.com">vquet@groupcls.com</a> ;
LEGOS	A. Cazenave ; L. Leclercq B. Meyssignac ; F. Birol; F. Nino; F. Leger; L Tolu	<a href="mailto:anny.cazenave@gmail.com">anny.cazenave@gmail.com</a> ; <a href="mailto:lancelot.leclercq@univ-tlse3.fr">lancelot.leclercq@univ-tlse3.fr</a> ; <a href="mailto:Benoit.Meyssignac@univ-tlse3.fr">Benoit.Meyssignac@univ-tlse3.fr</a> ; <a href="mailto:florence.biol@univ-tlse3.fr">florence.biol@univ-tlse3.fr</a> ; <a href="mailto:fernando.nino@ird.fr">fernando.nino@ird.fr</a> ; <a href="mailto:fabien.leger@univ-tlse3.fr">fabien.leger@univ-tlse3.fr</a> ; <a href="mailto:lana.tolu@univ-tlse3.fr">lena.tolu@univ-tlse3.fr</a> ;
NOC	S Jevrejeva ; A Wise	<a href="mailto:sveta@noc.ac.uk">sveta@noc.ac.uk</a> ; <a href="mailto:anwise@noc.ac.uk">anwise@noc.ac.uk</a> ;
DGFI-TUM	Marcello Passaro	<a href="mailto:marcello.passaro@tum.de">marcello.passaro@tum.de</a> ;

**List of Contents**

<b>1. Introduction .....</b>	<b>4</b>
<b>2. New version v3.0 with spatial extension (June 2025). ....</b>	<b>5</b>
<b>3. Preliminary validation of the v3.0 sea level trends with tide gauges .....</b>	<b>8</b>
<b>4. Scientific applications .....</b>	<b>9</b>
<b>5. New trend error estimates at local scale of virtual stations .....</b>	<b>11</b>
<b>6. References .....</b>	<b>16</b>



## 1. Introduction

The objective of this report is to summarize the ongoing inter comparison and validation results of the latest version (**version v3.0; June 2025**) sea level dataset generated during the extension of the ESA Sea Level Climate Change Initiative program (SL\_cci+). The goal is to certify the quality of the final datasets distributed to the users.

Different coastal sea level datasets have been produced since the beginning of the project:

(1) **version 1.1**, consisting of a 16-year-long (June 2002 to May 2018), high-resolution (20-Hz), along-track sea level dataset at monthly interval, together with associated sea level trends computed at 429 coastal sites in six regions (Northeast Atlantic, Mediterranean Sea, West Africa, North Indian Ocean, Southeast Asia and Australia). The validation of this v1.1 data set was presented in Benveniste et al., Coastal sea level anomalies and associated trends from Jason satellite altimetry over 2002-2018, *Nature Scientific Data*, 7, 357, <https://doi.org/10.1038/s41597-020-00694-w>, 2020.

(2) **version 2.0**, computed during autumn 2021. This is an extension both in time and space of version 1.1. It covers a full 18 year-long time span: January 2002 to December 2019, and in addition to the previous 6 study regions, now covers the whole African continent. This V2.0 product was further extended spatially to include the whole American continent. This geographically extended product is called **v2.1**. It has been presented in Cazenave et al., New network of virtual altimetry stations for measuring sea level along the world coastlines, *Nature Communications Earth and Environment*, 2022.

(3) **version 2.2**. It is an improved version of the v2.1 product with some corrections applied to the dry tropospheric correction (wrong at a few sites) and an optimized calculation of the inter mission bias. The v 2.2 product has been distributed (<https://doi.org/10.17882/74354>).

(4) **version 2.4**. Produced in November 2024, this new version still covers the 2002-2021 time span but differs from the previous v2.3 version by the following improvements: (i) the use of the new GDR-F altimetry standards for Jason-3. The ALES-based waveforms and associated SSB have been recomputed with these new standards for Jason-3; (ii) a new post-processing editing applied to the sea level anomalies time series produced by X-TRACK consisting of a new criteria of at least 50% of valid data over the duration of each Jason mission and an iterative removal of the outliers in the sea level anomalies time series (in addition of the editing criteria previously applied to the sea level trend computation). This product still uses the FES2014 ocean tide model. It consists of 1149 virtual stations.

In addition, the SL\_cci+ activity also focused on the characterization of the uncertainties of the regional sea level trends. The results were presented in Prandi et al., Local sea level trends, accelerations and uncertainties over 1993-2019. *Sci*



Data 8, 1 (2021). <https://doi.org/10.1038/s41597-020-00786-7>. This work has already been presented in previous issues of this report, and a dedicated publication is in preparation (Mangilli et al.).

Since then, a new approach has been developed to provide realistic uncertainties at the virtual stations. It is described in section 4.

## 2. New version v3.0 with spatial extension (June 2025).

In 2025, a new coastal sea level data set (version v3.0) has been produced. The time span of analysis (2002-2021) has remained the same as for previous versions. The v3.0 dataset differs from the previous v2.4 product (released in November 2024) by an important spatial extension. It also uses the new improved FES22 ocean tide model instead of FES14 model considered in the previous versions. Six new regions have been considered in addition to the 13 previously considered, with the latter sometimes extended spatially to cover new oceanic zones of interest. The newly covered areas include tropical islands of the Pacific and Indian oceans, the New Zealand area, the Red Sea, the Baltic Sea and the northwest Pacific around Japan. The location of the new 19 regions is shown in Figure 1.

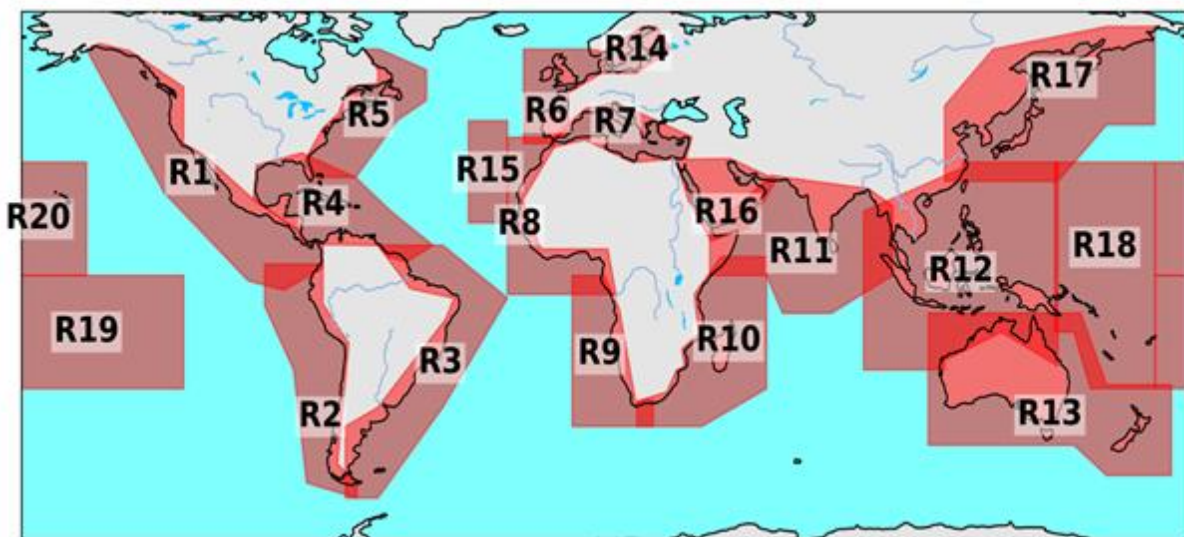


Figure 1- Map of the 19 regions covered by the along-track coastal sea level product of version 3.0.

The v3.0 version now consists of a set of 1634 virtual stations. The location and distribution in terms of distance to the coast is shown in Fig.2.

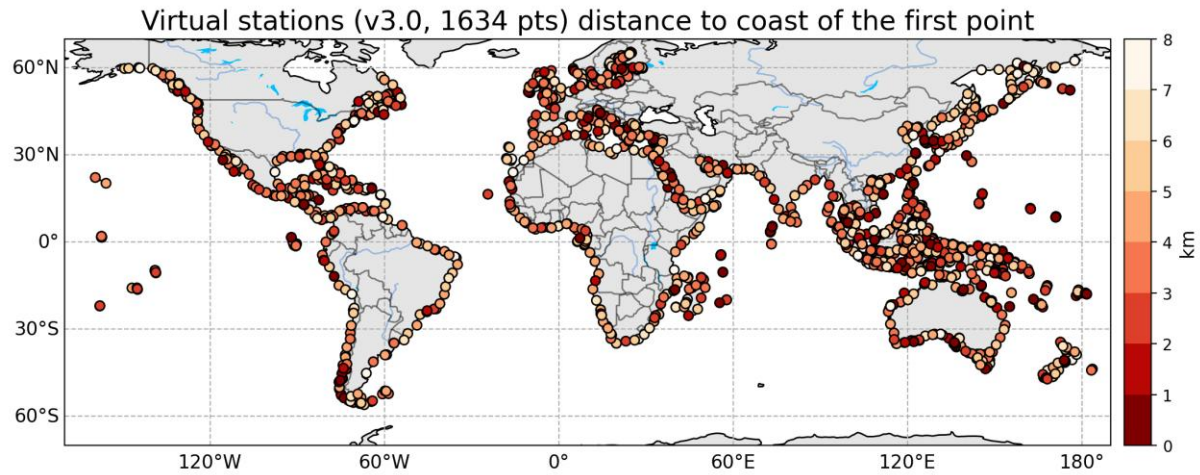


Figure 2: Location of 1634 virtual stations located at less than 8 km from the coast (V3.0 product)

In Figure 3 are also shown the location of the 596 virtual stations located at less than 3 km from the coast. On the map are also shown the tide gauge sites with at least 80% of valid data over the 2002-2021 time span.

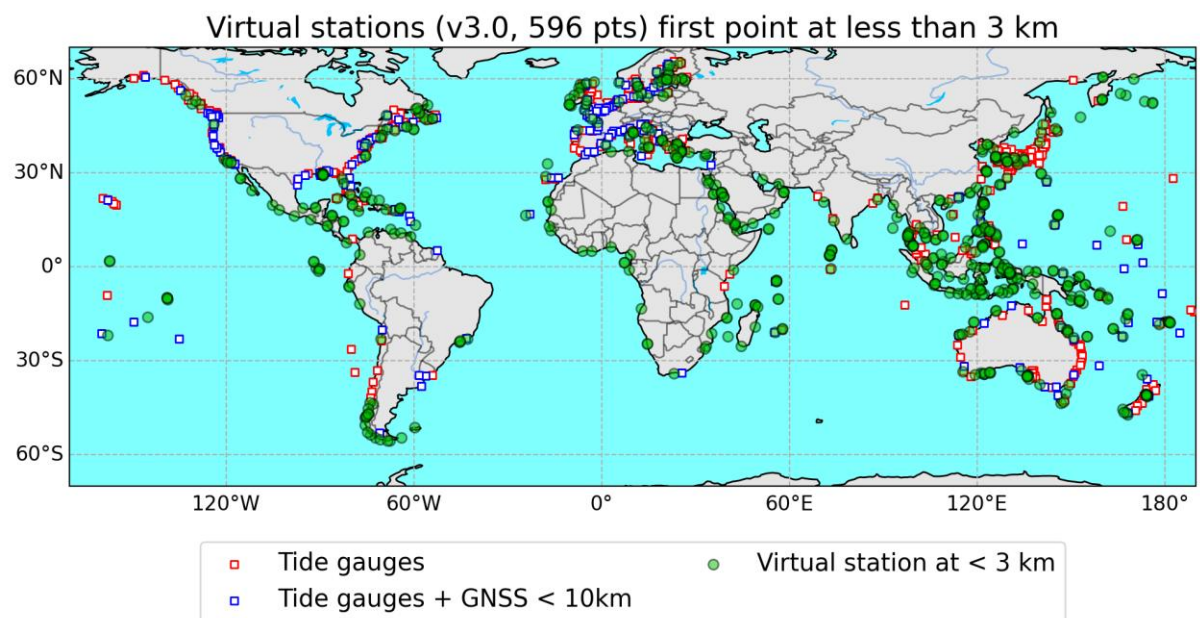


Figure 3 Location of virtual stations (green dots) located at less than 3 km from the coast (V3.0 product). The squares (blue/red) represent the tide gauge sites with records of at least 80% of valid data over the 2002-2021 time span with/without a GNSS station located at less than 10 km.

Figure 4 shows the distribution of the computed trends and associated errors, as well as distance to coast of the virtual stations. The average distance of the first valid point for the whole set of 1634 virtual stations is 3.7 km with 399 sites at less than 2 km and 596 sites at less than 3 km from the coast. We also note that an important number of virtual stations are at less than 1 km from the coast. This mostly occurs in the small tropical islands. The average trend error is about 1 mm/yr but it is based





on the least-squares fit of a linear trend to the monthly sea level time series. More realistic errors are provided in section 4.

Histogrammes of all dataset 3.0

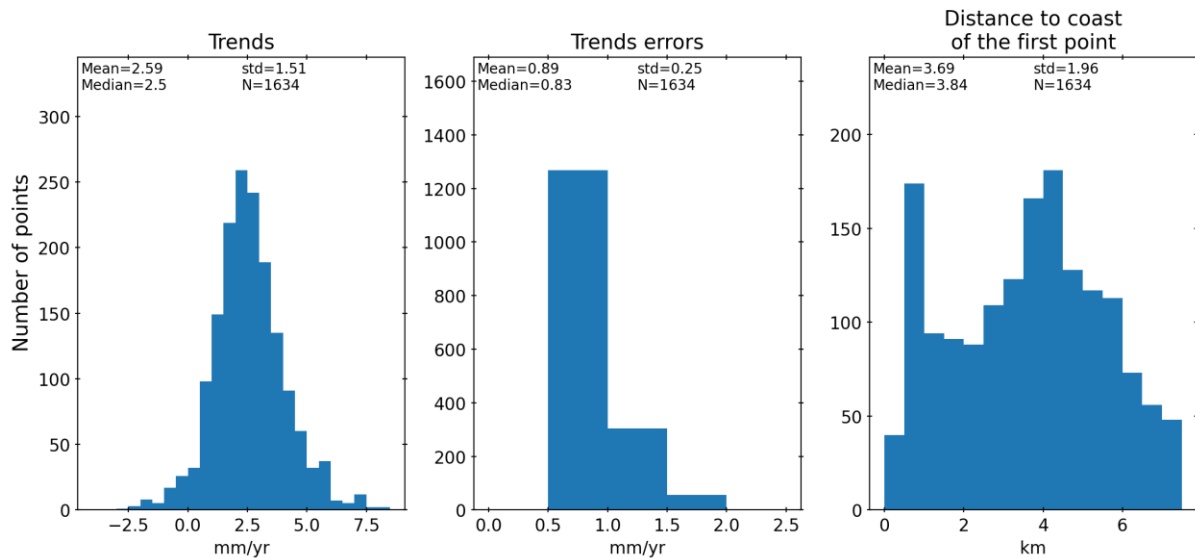


Figure 4 - Histograms of trends, trend errors and distance to the coast of the 1634 virtual stations (v3.0 product)

Two examples of sea level anomaly time series (averaged over the first 10 along-track points) and sea level trends against distance to the coast are shown in Fig.5 for the Seychelles and Maldives islands in the Indian ocean (v3.0 product).

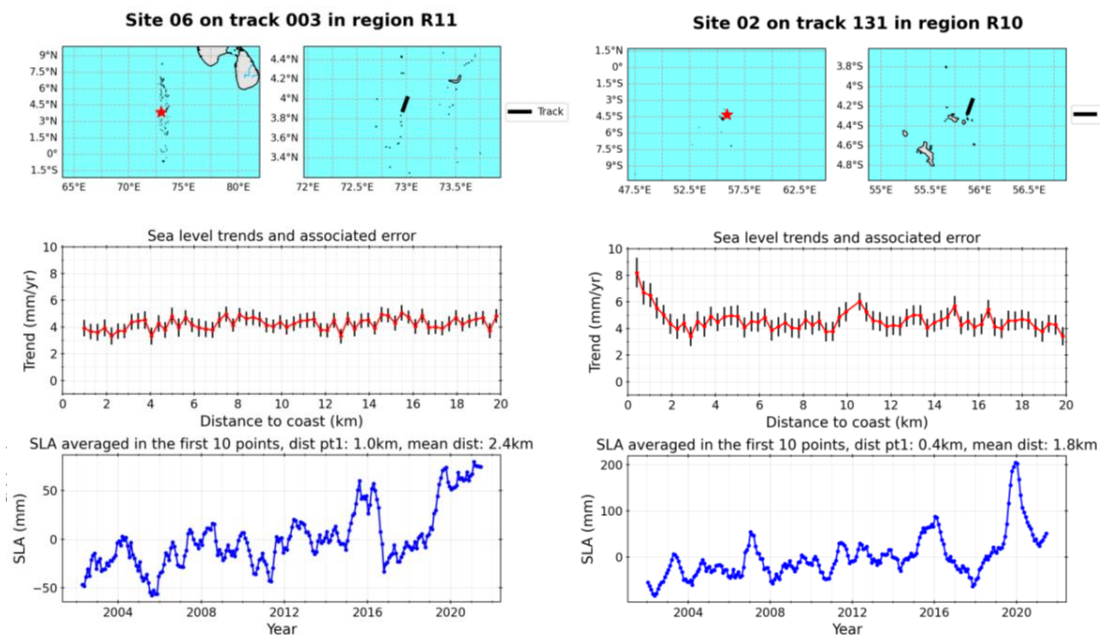


Figure 5 - Examples of sea level anomaly time series (averaged over the first 10 along-track points; blue curves) and sea level trends against distance to the coast (red points) (v3.0)



product). Left panel: Seychelles Islands (Indian Ocean). Right panel: Maldives islands (Indian Ocean).

### 3. Preliminary validation of the v3.0 sea level trends with tide gauges

A comparison of the altimetry-based sea level anomaly time series (version v3.0) at virtual stations with tide gauge records has been performed at the set of 372 sites for which the tide gauge is located at less than 50 km from the virtual station, and the tide gauge record has at least 80% of valid data over the studied time span (2002-2021). 114 out of 372 are collocated with a GNSS station (at less than 10 km). This allows to estimate vertical land motion (VLM) at the tide gauge, hence after correcting the tide gauge-based relative sea level trend from the VLM, this allows to estimate the absolute sea level trend at the tide gauge and compare with the altimetry-based coastal sea level trend. For this purpose, an average over 10 successive points from the closest point to coast are considered.

Fig.6 below shows the 372 tide gauge sites.

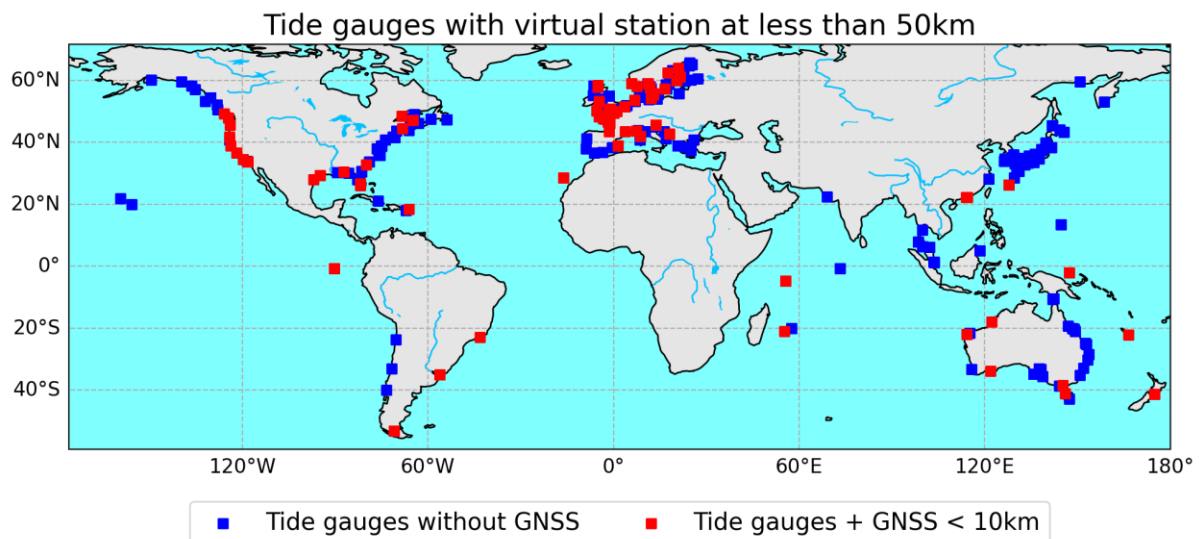


Figure 6 - Map of the 372 tide gauges located at less than 50 km from a virtual station (v3.0 product). Red squares correspond to tide gauges with a GNSS station at less than 10 km.

Figure 7 shows two examples of coastal sea level time series with tide gauge record superimposed. Correlations between both time series are also indicated.

Correlations are generally high ( $>0.8$ ) in most regions, except in areas where the sea level time series are subject to strong high frequency (subseasonal) variability (e.g., Northwestern Europe, Adriatic Sea, Tasmania) where the correlation is significantly lower.



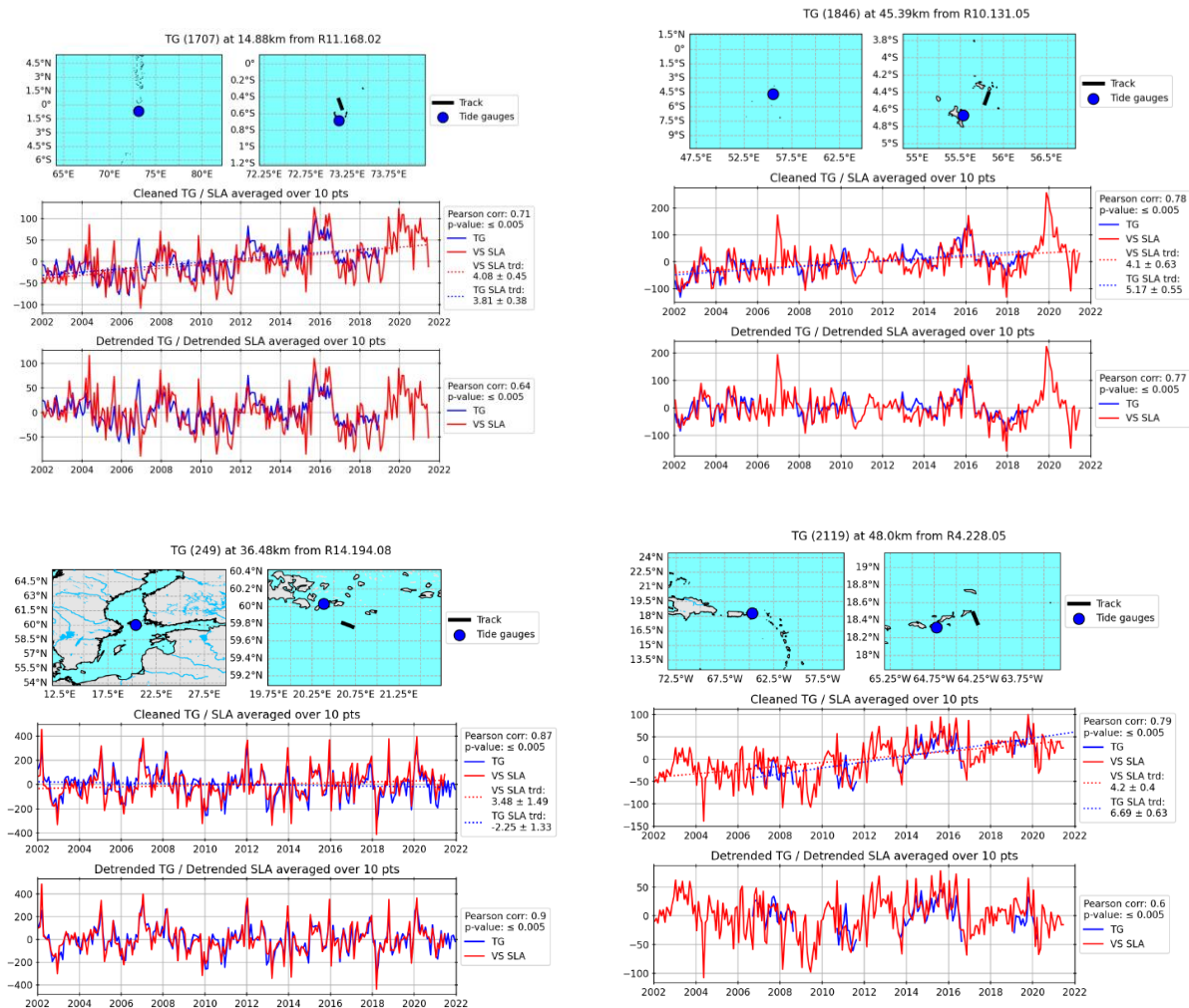


Figure 7 - comparisons of sea level time series at virtual stations with tide gauge record. (a) Maldives; (b) Seychelles islands; (c) Baltic Sea; (d) Caribbean islands.

While a primary purpose of the comparison between the altimetry-based coastal sea level data with tide gauge records was to validate the v3.0 product, from Figure 7, we note that the coastal sea level data are mostly useful to fill the gaps in the tide gauge records (Caribbean island case), or to extend them (Seychelles and Maldives islands). This is also obviously true at virtual coastal sites where there is no tide gauge.

## 4. Scientific applications

The coastal sea level products have been used in three recent scientific publications:

1. Leclercq L, Dieng H., Cazenave A. et al., Spatio-temporal changes in interannual sea level along the world coastlines, *Global and Planetary Change*, 253, 104972, <https://doi.org/10.1016/j.gloplacha.2025.104972>, 2025.

**Abstract:** To investigate how coastal sea level evolves at interannual time scales from one region to another, we perform an Empirical Orthogonal Function (EOF)



*decomposition of coastal sea level time series derived from reprocessed coastal altimetry data over a 20-year long time span (2002-2021), at 1132 virtual coastal stations homogeneously distributed along the world coastlines. This analysis is first performed globally and then over selected coastal regions. Consistent with previous studies, the results show the dominant influence of internal climate modes, in particular ENSO (El Niño Southern Oscillation), on the interannual coastal sea level variability. But our study also reports novel findings in coastal sea level: (1) a regime shift between 2008 and 2012, with increased sea level rate after that date in many coastal regions, and (2) a 6-year cycle, notably along the northeast and northwest coasts of America (north of 40 ° N) and along the Indian coast of Indonesia. Additional EOF analyses are done using both gridded altimetry sea level data from the Copernicus Climate Change Service and an ensemble mean of four ocean reanalyses, in three successive coastal bands: 0-50 km, 50-100 km and 100-500 km from land. They confirm the strong influence of internal climate modes at the coast but also show that results in the cross-shore direction towards the open ocean are similar to those at the coast. This study based on three different datasets shows that the strong influence of internal climate modes on sea level interannual variability in the world coastal zones is not limited to the open ocean but also dominates sea level changes very close to the coast. It also shows evidence of a regime shift in the rate of change of coastal sea level between 2008 and 2012 and the presence of a 6-year oscillation in coastal sea level, possibly linked to the recent discovery of a 6-year cycle in the whole climate system.*

**2. Leclercq L., Cazenave A. et al., Coastal sea level rise at altimetry-based virtual stations in the Gulf of Mexico, *Advances in Space Research*, 75, 1636-1652, <https://doi.org/10.1016/j.asr.2024.11.069>, 2025.**

**Abstract:** A dedicated reprocessing of satellite altimetry data from the Jason-1/2/3 missions in the world coastal zones provides a large set of virtual coastal stations where sea level time series and associated trends over 2002-2021 can be estimated. In the Gulf of Mexico, we obtain a set of 32 virtual coastal sites, well distributed along the Gulf coastlines, completing the tide gauge network with long-term data that is currently limited to the northern part of the Gulf. Altimetry-based coastal sea level time series and associated sea level trends confirm previous published results that report a strong acceleration in tide-gauge based sea level rise along the US coast of the Gulf of Mexico since the early 2010s. In addition, our study shows that this acceleration also takes place along the western and southern coasts of the Gulf of Mexico. The coastal sea level trends estimated over 2012-2021 amounts to 10 mm/yr at most virtual stations. We note a slightly smaller rise on the western coast of Florida and at two sites of the Cuba Island. Good agreement in terms of sea level trends over 2002-2021 is found between coastal altimetry data and tide-gauge records corrected for vertical land motions. Good correlation is also found between coastal altimetry and tide gauge sea level time series at low-frequency time scales, with interannual fluctuations in sea level being indirectly linked to natural climate modes, in particular the El Niño-Southern Oscillation (ENSO).

**3. Cazenave A., R. Almar, P. Almeida, N. K. Ayoub, J. Bettencourt, F. Birol, W. Han, M. Herrmann, S. Jevrejeva, L. Leclercq, F. Niño, J. Oelsmann, F. Papa, S. Ponce de León, A. Tarpanelli, V.D. Vinh. Present-day sea level variations in**



## coastal areas from daily to multi-decadal time scales; Observations and causes. Submitted, Surveys in Geophysics, 2025.

**Abstract:** *Sea level changes near the coast may deviate from what we observe in the open ocean. In effect, these changes result from the superposition of the climate-related global mean rise and associated regional trends, plus local contributions related to processes specific to near-shore areas. The latter operate on a broad range of time scales, from subdaily to multi-decadal. They include ocean tides, atmospheric forcing, wind and waves, trapped coastal waves, coastal currents, river discharge in deltas and estuaries, natural climate modes and remote steric and mass effects. Changes in coastal ocean circulation driven by bathymetry, shape of coastal boundaries and changing forcing factors, can also impact coastal sea level. Such coastal processes not only directly produce coastal sea level changes, but also mediate the coastal response to open-ocean forcing. Vertical crustal motions are an additional factor causing sea level to vary with respect to the ground, in a proportion often larger than climate-related sea level changes. Due to all involved processes, coastal sea level can significantly vary from one region to another. Here we first discuss how coastal sea level is measured by in situ and space-based observing systems. Next, we review all processes causing sea level variations at the coast, from high-frequency extreme events to long-term, multidecadal changes. We also discuss different types of models developed for process understanding. Finally we propose a number of recommendations for extending in space and time both in situ and space-based observations of coastal sea level changes, including vertical land motions and other forcing factors, and for developing adequate models for improved process understanding.*

### 5. New trend error estimates at local scale of virtual stations

The new error estimates for trend calculations at virtual stations are calculated using an extension of the methodology of Prandi et al (2021). The complete method will be described in the ATBD document of this project, but it is useful to keep in mind that the main difference with Prandi's general method is that we use along-track, high-rate data (instead of global  $2^\circ \times 2^\circ$  grids). Because of this we have more precise data, but this means we also have to deal with missing data.

As in Prandi et al's work, we define uncertainties as the sum of drift, bias and noise components. Drift and bias calculations are mostly unchanged from their work, but the noise component is completely different.

The noise component is estimated using the square root of the diagonal of the variance-covariance matrix of a set of SLA calculations. In essence, these variance elements are calculated from the cartesian product of a set of available corrections, as listed in Table 1 and Table 2 below.



J2	
CORRECTION	SOLUTION
orbit	orbit.alti.poe_gdr_e
range	range.ales_2025
dac	mog2D + inverse_barometer_from_rads
dry	dry_tropospheric_correction.model.ecmwf
	dry_tropo era5
	dry_tropo ncep
iono	ionospheric_correction.alti.xtrack_filtered
	ionospheric_correction.alti.rtk_adaptive
	ionospheric_correction.model.gim
wet	wet_tropospheric_correction.gpd_plus_j2
	wet_tropospheric_correction.rad
	wet tropospheric correction.model.ecmwf
tide	ocean_tide_height.model.fes22
	ocean_tide_height.model.fes14b
	ocean_tide_height.model.got4v10
	ocean_tide_height.model.eot20
mss	mean_sea_surface.model.cnescls15
	mean_sea_surface.model.cnescls21.ctoh_j2
	mean_sea_surface.model.sio.ctoh_j2
ssb	sea_state bias.alti.ales_2025

*Table 1 - Set of corrections used to calculate SLA for the J2 mission*



J3	
CORRECTION	SOLUTION
orbit	orbit.alti.cnes_poe_f
range	range.ales_2025
dac	mog2D + inverse_barometer_from_rads
dry	dry_tropospheric_correction.model.ecmwf
	dry_tropo era5
	dry_tropo ncep
iono	ionospheric_correction.alti.xtrack_filtered
	ionospheric_correction.alti.rtk_adaptive
	ionospheric_correction.model.gim
wet	wet_tropospheric_correction.gpd_plus_j3
	wet_tropospheric_correction.rad
	wet tropospheric correction.model.ecmwf
tide	ocean_tide_height.model.fes22
	ocean_tide_height.model.fes14b
	ocean_tide_height.model.got4v10
	ocean_tide_height.model.eot20
mss	mean_sea_surface.model.cnescls15
	mean_sea_surface.model.cnescls21.ctoh_j3
	mean_sea_surface.model.sio.ctoh_j3
ssb	sea_state_bias.alti
	sea_state bias.alti.ales_2025
	sea_state_bias.alti.adaptive proto
	sea_state bias.alti.update

Table 2 - Set of corrections used to calculate the SLA of the J3 mission

If we use all possible SLAs using these altimeter corrections, we can generate 324 different calculations of SLA for J2 and 1296 for J3. The objective is to compute a noise value based on the variability of corrections relative to each other. For each along-track point of the station, we compute 2 noise values, one for J2 (also used for J1 period), and one for J3. We consider that the standard deviation of the variances of pairwise differences in the different SLAs is a proxy for the noise component of the uncertainty values. Once we have these values, we can then compute the variance covariance matrices (one per along track point of the station), and derive the trend confidence interval, following Prandi et al.'s methodology, and associate, for each along track point of each virtual station, an uncertainty on the trend of SLA.

To date, the results are available for a total of 1634 virtual stations. The trend confidence interval (CI) histogram of these stations is given for what we call the C0v6 estimation. Three subsets are studied: all stations (1634 stations), stations where at least one along-track point has a trend CI greater than 3 mm/yr (102 stations) and the subset of stations where at least one along-track point has a trend CI greater than 6 mm/yr (20 stations). They are shown in Figure 8 below. In these



histograms, all the along-track points of the stations are included (up to 20km from the coastline), even those which have a CI below 3 or 6 mm/year. This means that if one along-track point of the station has a trend CI above 3 mm/year, all the along-track points of the station are represented in the histogram.

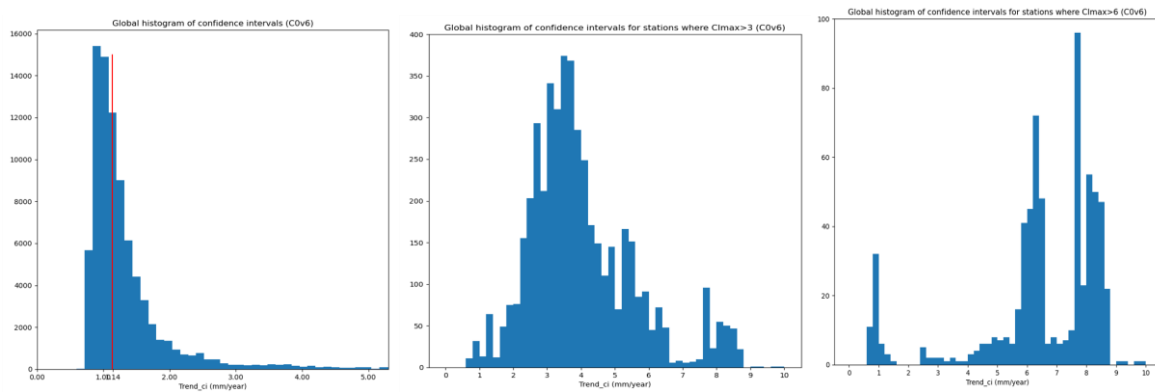


Figure 8 - Histogram of (a) all stations (b) stations with trend CI > 3 mm/yr (c) trend CI > 6 mm/yr

Illustrated on a map, we can look at the CI on SLA trends for each station. However, because we work with high-rate (20Hz) data, each virtual station has several along-track points. We thus plot the mean trend CI for these points at each virtual station, in Figure 9. As before, we also plot the subsets of stations with trend CI > 3 mm/yr and trend CI > 6 mm/yr in Figure 10, and Figure 11 respectively.

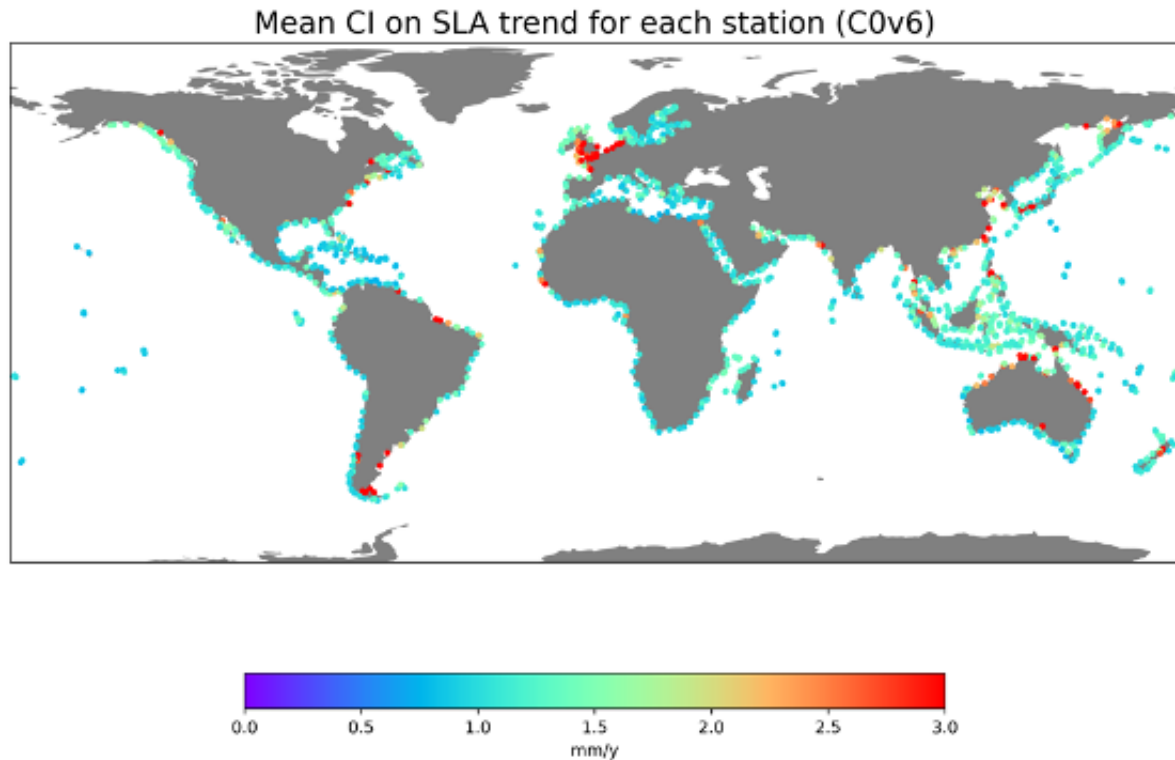
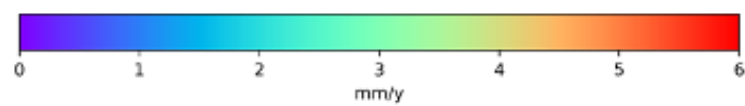
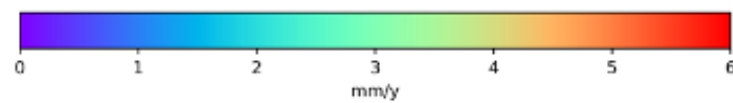


Figure 9 - Mean trend CI for all stations



Mean CI on SLA trend for each station where  $CI > 3\text{mm/y}$  (C0v6)*Figure 10 - Mean trend CI for stations with  $CI > 3\text{mm/yr}$* Mean CI on SLA trend for each station where  $CI > 6\text{mm/y}$  (C0v6)*Figure 11 - Mean trend CI for stations with  $CI > 6\text{mm/yr}$*



The reason for analyzing the results of the two subsets with high trend confidence intervals is precisely that: the intervals are unrealistically high. Additional work has shown that these cases arise in virtual stations whose settings are in difficult geographical configurations: along a peninsula, in sheltered areas surrounded by land, and other configurations that are suboptimal for altimetry estimations.

For the time being, 94% of all virtual stations contain satisfactory values, and can thus be published. The remaining 6% (102 stations), will also be included in the published product, but the project has chosen to include a product flag, indicating that the quality of data is not the best. This product should be published in 2026, but in the meantime additional work is underway to better understand the behavior of the high-trend CI virtual stations.

## 6. References

- Ablain M, Meyssignac B, Zawadzki L, Jugier R, Ribes A, Cazenave A, Picot N. 2019. Uncertainty in satellite estimate of global mean sea level changes, trend and acceleration, *Earth Syst Sci Data*. 11:1189-1202. DOI:10.5194/essd-11-1189-2019.
- Benveniste et al., Coastal sea level anomalies and associated trends from Jason satellite altimetry over 2002-2018, *Nature Scientific Data*, 7, 357, <https://doi.org/10.1038/s41597-020-00694-w>, 2020.
- Cazenave A. and the Climate Change Initiative Coastal Sea Level Team, Sea level along the world's coastlines can be measured by a network of virtual altimetry stations, *Nature Communications, Earth & Environment*, 3, 117, <https://doi.org/10.1038/s43247-022-00448-z2022>, 2022.
- Cazenave A., R. Almar, P. Almeida, N. K. Ayoub, J. Bettencourt, F. Birol, W. Han, M. Herrmann, S. Jevrejeva, L. Leclercq, F. Niño, J. Oelsmann, F. Papa, S. Ponce de León, A. Tarpanelli, V.D. Vinh. Present-day sea level variations in coastal areas from daily to multi-decadal time scales; Observations and causes. Submitted, *Surveys in Geophysics*, 2025.
- Chib S. (1993) Bayes regression with autoregressive errors. A Gibbs sampling approach *J. Econometrics*, 58, pp. 275-294.
- Dieng H.B., Cazenave A., Gouzenes Y. and Sow, A., Trends and inter-annual variability of coastal sea level in the Mediterranean Sea: Validation of high-resolution altimetry using tide gauges and models, 68, Issue 8, 3093-3520, *Advances in Space Research*, 2021.
- Gouzenes Y, Leger F. Cazenave A., Birol F., Almar R., Bonnefond P., Passaro M., Legeais J.F. and Benveniste J., Coastal sea level change at Senetosa (Corsica) during the Jason altimetry missions, 16, 1-18, 2020 <https://doi.org/10.5194/os-16-1-2020>, *Ocean Sciences*, 2020.
- Holgate, S. J. et al. New data systems and products at the permanent service for mean sea level. *J. Coast. Res.* 29, 493-504 (2013).
- Leclercq L, Dieng H., Cazenave A. et al., Spatio-temporal changes in interannual sea level along the world coastlines, *Global and Planetary Change*, 253, 104972, <https://doi.org/10.1016/j.gloplacha.2025.104972>, 2025.
- Leclercq L., Cazenave A. et al., Coastal sea level rise at altimetry-based virtual stations in the Gulf of Mexico, *Advances in Space Research*, 75, 1636-1652, <https://doi.org/10.1016/j.asr.2024.11.069>, 2025.



- Peltier W.R 2004 Global Glacial Isostasy and the Surface of the Ice-Age Earth: The ICE-5G(VM2) model and GRACE. *Ann. Rev. Earth. Planet. Sci.* 2004. 32,111-149.
- Prandi, P., Meyssignac, B., Ablain, M., Spada, G., Ribes, A. & Benveniste, J., Local sea level trends, accelerations and uncertainties over 1993-2019. *Sci Data* 8, 1 (2021). <https://doi.org/10.1038/s41597-020-00786-7>
- Prichard, D., and J. Theiler (1994), Generating surrogate data for time series with several simultaneously measured variables, *Phys. Rev. Lett.*, 73, 951-954.
- Rasmussen, C. E., C. K. I. Williams, *Gaussian Processes for Machine Learning* (MIT Press, Cambridge, MA, 2006).
- Tozer B., Sandwell D. Smith W. et al., Global Bathymetry and Topography at 15 Arc Sec: SRTM15+, Earth and Space Sciences, <https://doi.org/10.1029/2019EA000658>, 2019.
- Woodworth, P.L., Melet, A., Marcos, M. et al. Forcing Factors Affecting Sea Level Changes at the Coast. *Surv. Geophys.* 40, 1351-1397 (2019). <https://doi.org/10.1007/s10712-019-09531-1>
- Wöppelmann, G., and M. Marcos (2016), Vertical land motion as a key to understanding sea level change and variability, *Rev. Geophys.*, 54, 64-92, doi:10.1002/2015RG000502.

End of the document